

Liquid Crystal Transition and Crystallization Kinetics in Poly(ester imide)s

Ricardo Pardey, Scott S. Wu, Jianhua Chen, Frank W. Harris, and Stephen Z. D. Cheng*

Institute and Department of Polymer Science, The University of Akron, Akron, Ohio 44325-3909

Andrew Keller

H. H. Wills Physics Laboratory, University of Bristol, Bristol BS8 1TL, England

Jerry Aducci and John V. Facinelli

Department of Chemistry, Rochester Institute of Technology, Rochester, New York 14623-0887

Robert W. Lenz

Department of Polymer Science and Engineering, University of Massachusetts at Amherst, Amherst, Massachusetts 01003

*Received January 4, 1994; Revised Manuscript Received May 13, 1994**

ABSTRACT: A series of monotropic liquid crystal poly(ester imide)s (PEIMs) was synthesized from *N*-[4-(chloroformyl)phenyl]-4-(chloroformyl)phthalimide and nine diols containing 4–12 methylene units (*m*). During cooling from their isotropic melts, all the polymers underwent a monotropic liquid crystal transition to form a smectic A phase, followed by a transition to a more ordered structure, which was examined with wide-angle X-ray diffraction, differential scanning calorimetry, and polarized light microscopy. The fact that the liquid crystal transition temperatures for some of the PEIMs were close to their glass transition temperatures provided an opportunity for the study of liquid crystal transition kinetics in temperature regions close to the glass transition temperature. It was found that when the temperature, and thus the molecular mobility decreased, the transition time increased despite the fact that this transition is close to equilibrium. The crystallization kinetics of PEIM(*m*)s from both the liquid crystal phase and the isotropic melt were also studied. In PEIM(*m*=even)s (except for *m* = 4), two different ordered structures can be formed. One is a crystalline phase formed directly from the isotropic melt, and the other is a highly ordered mesophase having a hexagonal-like packing develop from the liquid crystal state. Only one crystal structure in PEIM(*m*=odd)s is observed. Special attention has been paid to the effect of the presence of liquid crystal order on the crystallization kinetics. The pronounced acceleration of the crystallization was observed whenever this was preceded by liquid crystal formation, an effect pertaining within a wide temperature range from close to T_m down to T_g .

Introduction

An enormous effort on understanding the transition behavior of liquid crystal polymers has been made since the synthesis of main-chain liquid crystal polymers became possible.¹ It has been known that one kind of mesophase, liquid crystal transitions from the isotropic melt, usually exhibits a first-order transition and occurs close to equilibrium (cooling rate independence). Such transitions can be easily determined through differential scanning calorimetry (DSC). Structural change during the transition can be characterized via wide-angle X-ray diffraction (WAXD) powder experiments. In nematic liquid crystal transitions, only a shift in the *d*-spacing of the average lateral distance between chain molecules is found, while for smectic A and C transitions, a sharp diffraction peak in the low-angle region appears and represents the layer spacing in the smectic phase. For higher ordered smectic or columnar phases WAXD diffraction peak(s) can also be observed in the wide-angle region. WAXD fiber patterns obtained from oriented samples are essential for distinguishing a three-dimensional crystal packing from highly ordered smectic phases. They also provide further information about the detailed lateral chain packing, layer

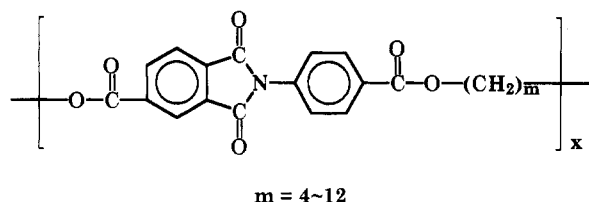
structure, and order correlations. Polarized light microscopy (PLM) is a unique experimental method to study liquid crystal order and morphology. In some cases, quantitative descriptions of defects may be obtained. For the semicrystalline polymers having a liquid crystal state, the "lamellar decoration" method using transmission electron microscopy (TEM)^{2–4} has been developed to establish relationships between molecular characteristics, such as chain rigidity, molecular weight, and Frank constants. Molecular motions in the liquid crystal and solid states have also been investigated via carbon-13 solid state nuclear magnetic resonance (NMR). During the last 3 decades, thermodynamic properties and morphological identifications of the main-chain liquid crystalline polymers have been progressively understood.

The isothermal transition kinetics of the liquid crystal phase from the isotropic melt is generally difficult to study since this transition is, in most of the cases, cooling rate independent in both transition temperatures and heats of transition and occurs close to equilibrium. The kinetics is not easily experimentally accessible for investigation. A few reports have dealt with liquid crystal transition kinetics or, more generally, mesophase transition kinetics from the isotropic melt. Examples are polyphosphazenes,⁵ polysiloxanes,⁶ 1,4-polybutadiene (trans),⁷ poly(tetrafluoroethylene),⁷ bis(4-hydroxyphenoxy)-*p*-xylene-based polyesters,⁸ poly(azomethine ether)s,⁹ poly(decamethylene-

* To whom correspondence should be addressed.

© Abstract published in *Advance ACS Abstracts*, September 1, 1994.

Chart 1
POLY(ESTER IMIDE)S (PEIM)



4,4'-diphenoxy terephthalate),¹⁰ and a few aromatic polyesters and copolyesters.¹¹⁻¹³ In all the cases reported, the transition kinetics is assumed to be nucleation-controlled and the overall kinetics is usually studied via the Avrami treatment.¹⁴ A generalization of the liquid crystalline transition kinetics from the isotropic melt is not achieved.

Mesophases can be classified as enantiotropic or monotropic. In the monotropic case, the mesophase is metastable throughout the whole temperature range. Nevertheless, it may become observable on cooling because crystallization, which is the transition to the state of ultimate stability, requires much larger supercooling and may therefore be bypassed. This behavior was recognized as early as in 1877.¹⁵ In 1923, over 100 liquid crystal molecules had been found to possess the monotropic transition behavior.¹⁶ Recently, this monotropic behavior has also been observed in main-chain liquid crystal polymers.¹⁷⁻²⁴

The large supercooling necessary for crystallization in a monotropic liquid crystalline polymer provides an additional opportunity to investigate the crystallization processes from both the liquid crystal phase and the isotropic melt. The comparison of these two kinetic behaviors may lead to a new understanding of the effect of the presence of liquid crystal order on the crystallization and of the relationship between the formation of the liquid crystal and crystal phases. For this purpose, a series of poly(ester imide)s has been synthesized from *N*-[4-(chloroformyl)phenyl]-4-(chloroformyl)phthalimide and nine diols containing 4-12 (*m*) methylene units. They can be abbreviated as PEIM(*m*) where *m* is the number of methylene units. The chemical structure for this series of polymers is shown in Chart 1. From our previous study,²⁵⁻²⁷ it has been recognized that PEIM(*m*)s show monotropic liquid crystal behavior with a smectic A order being identified during cooling. This series of PEIMs has also been synthesized in Professor Kricheldorf's research group.²⁸⁻³³ They have also reported that PEIMs form a crystal state with a layered supermolecular order, a so-called crystalline smectic state. In addition, PEIM-(*m*=even)s can form a smectic glass. After crystal melting, all PEIMs exhibit the isotropic state.

We have also found that the kinetics involving the liquid crystal transition in this series of polymers possesses an experimentally accessible temperature range. The reason is, as shown in Figure 1, that the liquid crystal transition temperature (T_d) is close to the glass transition temperature (T_g) in PEIM polymers particularly when *m* = odd. For example, PEIM(*m*=5) has a T_g of 364 K, which is higher than its T_d . No liquid crystal transition can thus be observed. For PEIM(*m*=7), the difference between these two transition temperatures ($T_d - T_g$) is 11 K. The difference in PEIM(*m*=9) is 34 K, and that in PEIM-(*m*=11) is 48 K. The liquid crystal transition window in these polymers is rather narrow. It is therefore possible to study the transition kinetics affected by the molecular

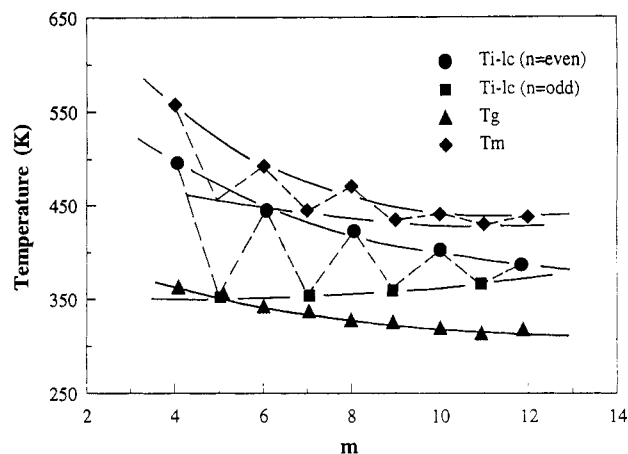


Figure 1. Liquid crystalline transition temperatures, glass transition temperatures, and melting temperatures for PEIMs.^{25,26}

Table 1. Inherent Viscosities of PEIM Polymers^a

PEIM(<i>n</i>)	η_{inh} (dL/g)	PEIM(<i>n</i>)	η_{inh} (dL/g)
4	0.40	9	0.62
5	0.50	10	0.61
6	0.52	11	0.60
7	0.65	12	0.59
8	0.60		

^a The inherent viscosities were measured in *m*-cresol at 303 K at a concentration of 0.5 %.

mobility, namely, the transport effect close to the glass transition temperatures. On the other hand, the difference between T_d and T_g is larger for PEIM(*m*=even)s. Thus for PEIM(*m*=4) it is 120 K, decreasing to 71 K for PEIM-(*m*=12).

Experimental Section

Materials and Samples. This series of poly(ester imide)s was synthesized from *N*-[4-(chloroformyl)phenyl]-4-(chloroformyl)phthalimide and the respective diols in refluxing 1,2,4-trichlorobenzene (TCB). The detailed synthetic route has been reported in a previous publication.²⁵ The polydispersity was estimated to be around 2-3. The inherent viscosities of the polymers are listed in Table 1. Sample weights prepared for DSC experiments were typically about 1 mg. Bulk samples for powder WAXD experiments were prepared by compressing the samples under pressure at high temperature to form films with a thickness of about 0.5 mm. Solution-cast films were used for PLM observations. The solvent was evaporated in a vacuum over at 520 K for 5 h. The thickness of solid films was about 10 μ m.

Instrumentation and Experiments. Differential scanning calorimetry (DSC) experiments were carried out on a Seiko DSC220. The temperature and heat flow scales were carefully calibrated using standard materials. Isothermal experiments were carried out for the kinetics study. The samples were heated above their melting temperature for 2 min and then shifted to the Seiko DSC220 which had been kept at a preset temperature. The instrument is equilibrated within 0.5 min. The data collection starts at the same time as the sample was switched into the DSC cell. The heat flow changes with time at constant temperatures were recorded.

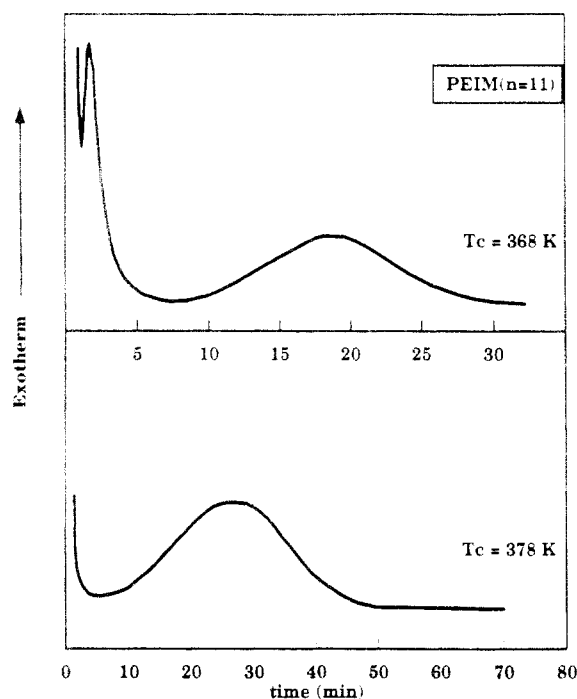
Wide-angle X-ray diffraction (WAXD) experiments were performed on a Rigaku 12 kW rotating anode generator (Cu K α radiation) with a diffractometer. A hot stage was set up on the diffractometer to measure the phase transition at different isothermal temperatures. The scanning 2θ angle region was between 2° and 35°. The thermal history of the samples is kept the same as those in the DSC experiments.

Polarized light microscopy (PLM) observations were obtained from an Olympus HB-2 with two Mettler hot stages FP-82 in order to carry out the isothermal experiments quenched from the isotropic melt.

Table 2. Thermodynamic Properties of the Liquid Crystal and Crystalline Phases in PEIMs

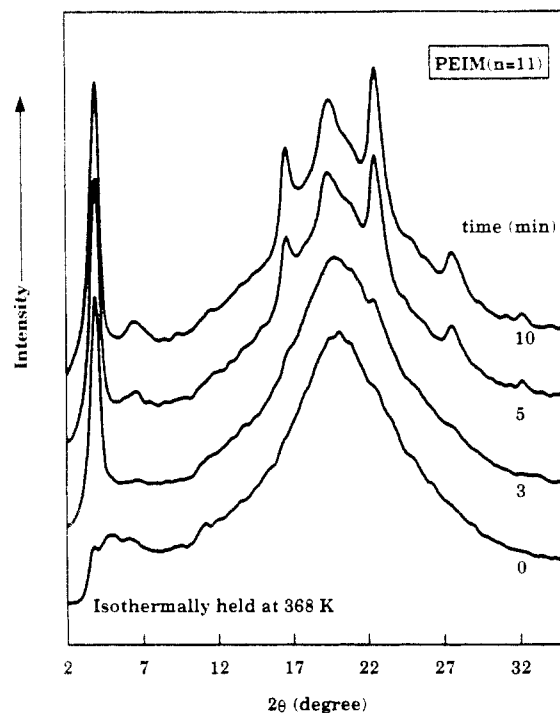
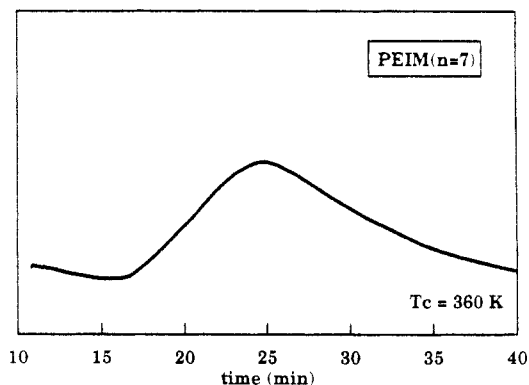
PEIM(<i>n</i>)	T_g (K)	T_d (K)	ΔH_d (kJ/mol)	$T_d - T_g$ (K)	T_m (K) ^a
4	380	500	3.1	120	558
5	364				
6	352	449	6.1	97	493
7	350	361	3.5	11	445
8	338	428	8.3	90	471
9	335	369	4.3	34	435
10	330	408	9.3	78	441
11	322	370	5.2	48	430
12	325	397	11.1	72	438

^a The melting temperatures were determined via T_m/T_c extrapolations. In PEIM(*n*=6, 8, 10, and 12), two crystal forms (I and II) exist (see text). The temperatures listed here are for the more stable form II. Melting temperatures of the less stable form I cannot be precisely determined since this crystal form converts to the more stable form II continuously.²⁶

**Figure 2.** DSC isothermal experiment for PEIM(*m*=11) at 368 and 378 K.

Results and Discussion

Identification of the Phase Transitions. Table 2 lists the liquid crystal transition temperatures and heats of transition for all PEIMs during cooling.^{25–27} The crystal melting temperatures, which were obtained based on T_m/T_c extrapolations, are also included in Table 2 and Figure 1.^{26,27} From isothermal DSC experiments, when the isothermal temperature is below the liquid crystal transition temperature (T_d), two exothermic transition processes are always observed for PEIMs. However, when the isothermal temperature is above the T_d , only one exothermic transition process is seen. For PEIM(*m*=odd)s, an example is PEIM(*m*=11). The first exothermic transition process in Figure 2 is completed at about 6–7 min at 368 K, which is below T_d . The second exothermic process starts developing at around 10 min. Therefore, it is necessary to study the ordering process before 6 min and after 10 min in order to identify the structural change in the polymer. Figure 3 shows time-resolved WAXD patterns for PEIM(*m*=11) at the same thermal history as in the DSC isothermal experiment. Before 5 min the only reflection peak is in the low-angle region at $2\theta = 3.40^\circ$ (*d*-spacing of 2.60 nm). The reflection peaks in the wide-angle region appear after 5 min. This indicates that the

**Figure 3.** WAXD isothermal experiment for PEIM(*m*=11) at 368 K for different times.**Figure 4.** DSC isothermal experiment for PEIM(*m*=7) at 360 K.

first exothermic transition observed in DSC experiments (Figure 2) is an ordering process of a smectic liquid crystal phase from the isotropic melt. The crystal structure develops during the second exothermic process. Similar results can be observed in PEIM(*m*=9) which has been described in one of our previous publications (Figure 4b in ref 25).

PEIM(*m*=7) apparently possesses only one exothermic transition process when the sample is isothermally kept at 360 K, as shown in Figure 4. This process seems to be completed after 60 min. The second transition process requires almost 1 day to develop, and the intensity of this exothermic process with time is too weak to be detected. Only successive heating experiments at different, interrupted isothermal times can provide the transition kinetics. To observe crystallization from the isotropic melt, times of several days to a week are necessary. The structural identification of the exothermic transition in Figure 4 is shown in Figure 5. It is clear that, after 8 min at 360 K, a low-angle reflection peak starts developing at $2\theta = 4.26^\circ$ (*d*-spacing of 2.07 nm). No reflection peak in the wide-angle region is observed. The intensity of the low-angle reflection peak increases with time until remaining constant after 64 min. Indeed, this slow ordering process is a liquid crystal transition from the isotropic melt. The

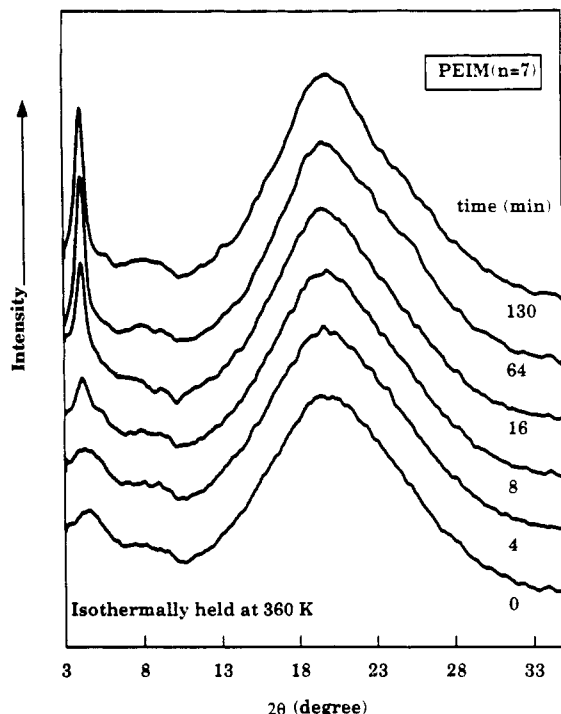


Figure 5. WAXD isothermal experiment for PEIM($m=7$) at 360 K for different times.

low-angle peak represents the layer spacing in this phase and identifies a smectic A phase as found through its quenched fiber pattern.²⁶ Only after hours of annealing time do the diffraction peaks in wide-angle region appear, revealing a further crystallization process in PEIM($m=7$). Although the liquid crystal transition is thermodynamically close to equilibrium, the transition kinetics can still be very slow due to hampered molecular motion since 360 K is only about 10 K above the glass transition temperature of PEIM($m=7$) (Figure 1).

WAXD experiments were also carried out at temperatures above the T_d for each of PEIM($m=\text{odd}$)s. The crystal structure (monoclinic lattices determined from WAXD fiber patterns²⁷ was found to be identical to that which develops below T_d (for example, in Figure 3 for PEIM($m=11$)), indicating that only one crystal structure exists in each of PEIM($n=\text{odd}$)s.

For PEIM($m=\text{even}$)s, as shown in Figure 6 for PEIM($m=12$), two exothermic processes are found when isothermally kept at 394 K ($T_d = 397$ K). The first one occurs within less than 1 min, and the second forms over 2–3 min. Although it is difficult to study the first transition kinetics of this polymer quantitatively, two exothermic processes are still evident. Only one transition process appears at 418 K with a peak time of around 22 min. The structural development can be monitored by WAXD as illustrated in Figure 7. When the isothermal temperature is 373 K, a clear low-angle reflection peak at $2\theta = 3.05^\circ$ (d -spacing of 2.89 nm) can be seen even for the shortest time (the layer spacing of the smectic A liquid crystal phase).²⁶ At wide angles only one sharp reflection peak develops at $2\theta = 20.0^\circ$ and occurs in the course of 1 min. This is the manifestation of a hexagonal-like lateral packing in PEIM($m=12$) developed below T_d . On the other hand, when the isothermal temperature is above T_d , the structural development is entirely different as evidenced by multi-reflection peaks as shown in Figure 8 at 395, 403, and 413 K. For the WAXD pattern at 395 K, residuals of the reflection peak at $2\theta = 20.0^\circ$ still remain, revealing a possibility of the coexistence of the two ordered structures. With increasing temperature, the intensity of the hex-

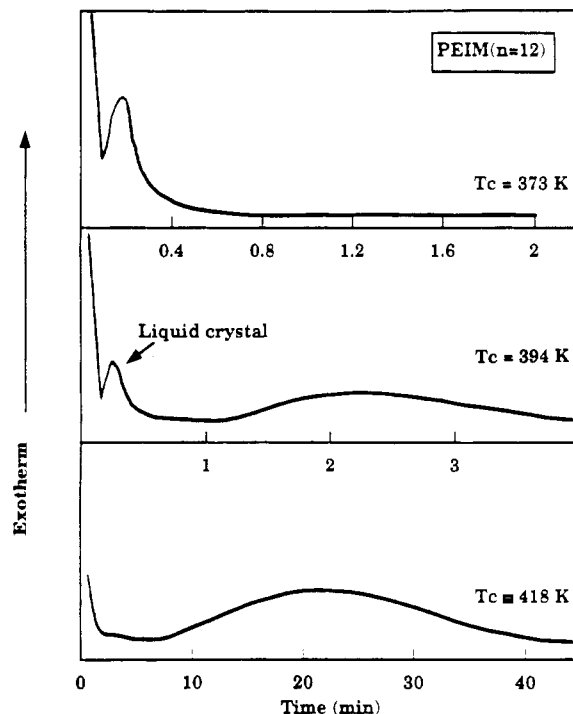


Figure 6. DSC isothermal experiment for PEIM($m=12$) at 373, 394, and 418 K.

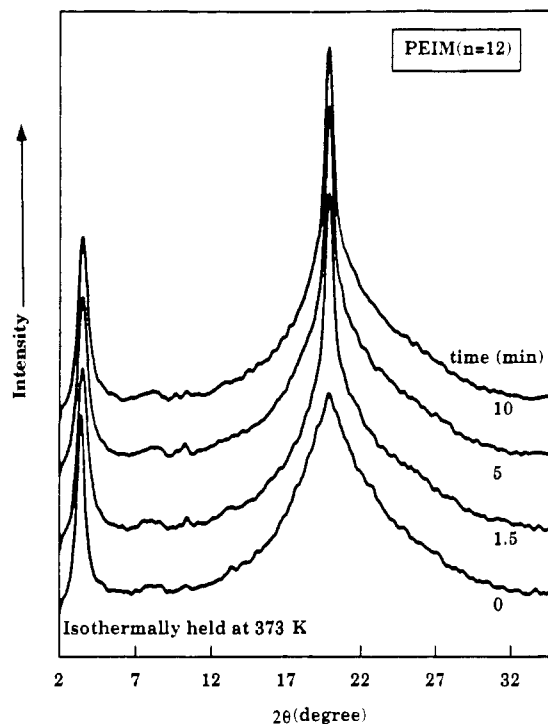


Figure 7. WAXD isothermal experiment for PEIM($m=12$) at 373 K for different times.

agonal-like structure decreases. This phenomenon can also be clearly seen in the case of PEIM($m=10$). Figure 9 shows WAXD patterns for this polymer at 403, 410, and 423 K ($T_d = 408$ K). At 403 K the WAXD result exhibits a clear major reflection peak at $2\theta = 20.0^\circ$. Other minor reflection peaks are attributed to a crystal structure which is the same as those which develop at higher temperatures. The formation of these peaks is due to the fact that quenching the PEIM($m=10$) sample is not fast enough to obtain a pure phase with the hexagonal-like structure.

PEIM($m=8$) possesses the same transition behavior as PEIM($m=10$) and $-(m=12)$. PEIM($m=6$) shows a difference in the ordered structure developed below the T_d .

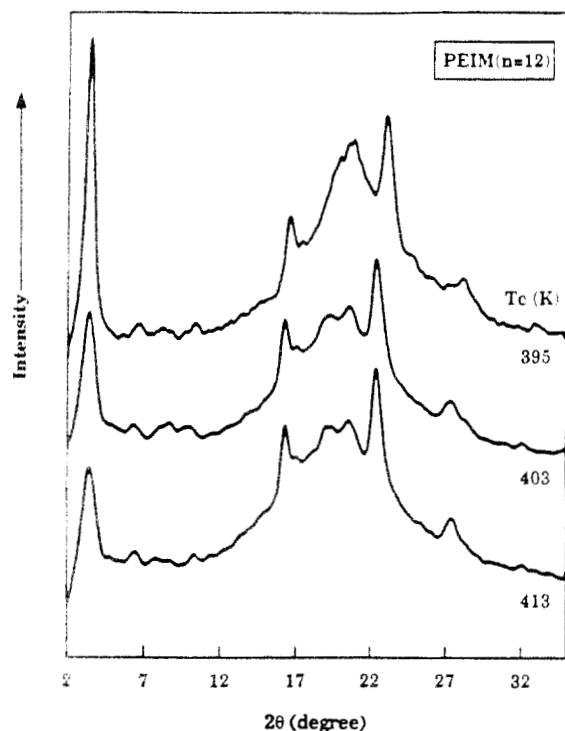


Figure 8. WAXD isothermal experiment for PEIM($m=12$) at 395, 403, and 413 K.

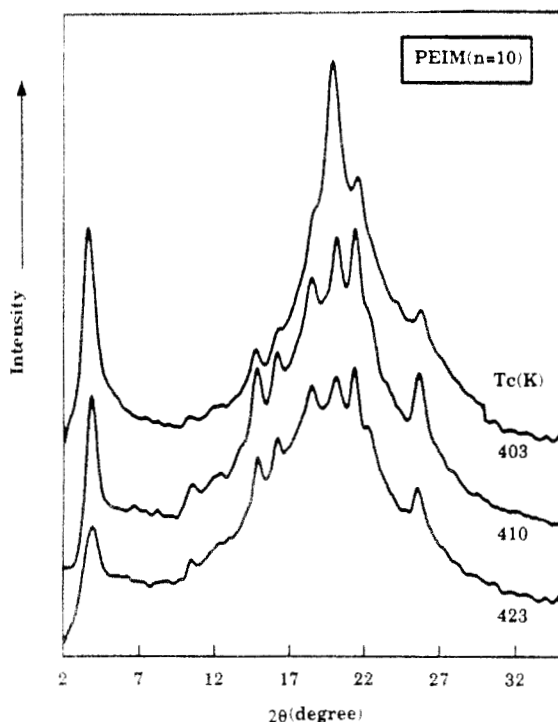


Figure 9. WAXD isothermal experiment for PEIM($m=10$) at 403, 410, and 423 K.

Instead of the hexagonal-like packing, this polymer possesses two major reflection peaks at $2\theta = 18.8^\circ$ and 23.0° (Figure 10). When the temperature is above the T_d , the second crystal structure (as for PEIM($m=8$, 10, and 12)) is found. For PEIM($m=4$), however, only one crystal structure exists in the entire temperature range below and above T_d .²⁷ For all PEIM($m=\text{even}$), the high-temperature crystal structures possess monoclinic lattices.²⁷ Isothermal PLM observations for PEIM($m=4$) at 518 K (above T_d) show that a crystal texture which fits to a broad concept of spherulites forms. The transformation seems to be athermal (heterogeneous). A fine-grained texture, char-

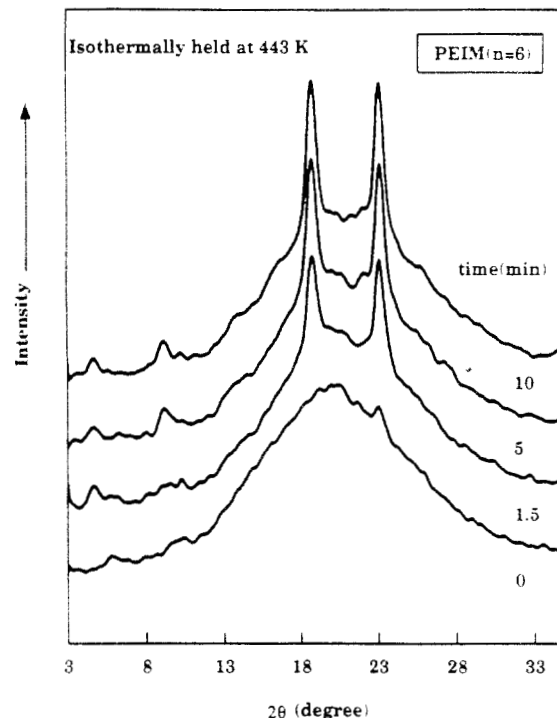
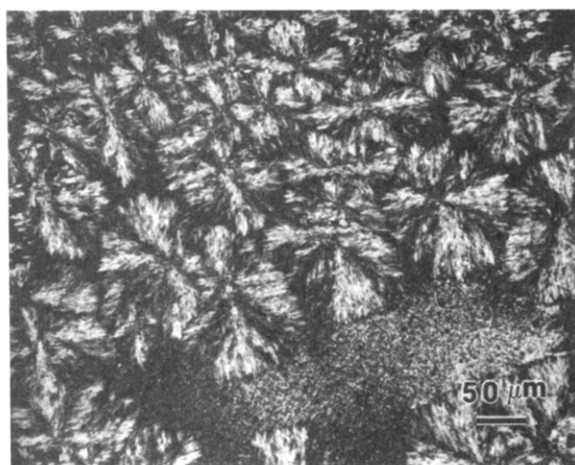
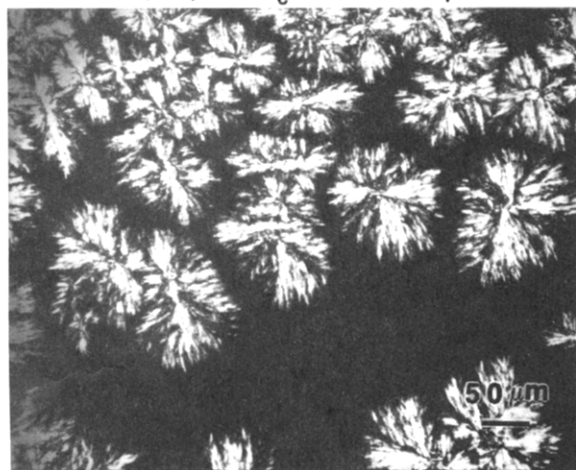


Figure 10. WAXD isothermal experiments for PEIM($m=6$) at 443 K.

acteristic of polymeric liquid crystals, appears during quenching to room temperature almost instantly (Figure 11). Subsequent reheating to 518 K leads to a melting of the liquid crystal phase at T_d (500 K) while the crystal textures remain (Figure 11). The latter melts at a higher temperature (T_m). Other PEIMs show observations similar to those of PEIM($m=4$). More detailed morphological changes with temperature and the number of methylene units will be reported elsewhere.

To summarize the experimental observations, below each T_d , it is clear that both even- and odd-numbered series show two exothermic transitions in isothermal experiments. The fast process is an isotropic melt to a smectic A liquid crystal phase transition, and the slow transition is a further ordering (crystallization) process. Regarding the slow transition process, for PEIM($m=\text{odd}$ s), only one crystal structure exists in the whole temperature range below and above T_d . In PEIM($m=\text{even}$ s), except for PEIM($m=4$), each polymer exhibits two different ordered structures. The less ordered structure (form I) is hexagonal-like for PEIM($m=8$, 10, and 12) below T_d . The crystal structure (form II) is monoclinic and formed above T_d . In the vicinity of the T_d , both structures may coexist. PEIM($m=6$) serves as an intermediate case between PEIM($m=4$) and other PEIM($m=\text{even}$ s) with higher numbered methylene units. Further annealing close to but below T_d may also lead form I to transform into form II. These results, again, indicate that, when an ordering process occurs, one or even several intermediate states may form before reaching the final ordered state. This phenomenon was already expressed by "Ostwald's law of successive states" which states that a phase will occur step-by-step through successively more stable polymorphs.³⁴

Liquid Crystal Transition Kinetics. The first try is the use of the Avrami treatment to fit the liquid crystal transition kinetic data as shown in Figures 12 and 13 ($\log[-\ln(1-w)]$ versus $\log(t)$ plots where w is the weight fraction of the ordered phase conversion). For PEIM($m=11$), two transition processes can be identified. The first process is rather fast and finished within a few

(a) PEIM (n=4) $T_c = 518$ K and quenched

(b) PEIM (n=4) reheated to 518 K

Figure 11. PLM observations of PEIM($m=4$) isothermally kept at 518 K for 60 min and quenched to room temperature (a) and then subsequently heated to 518 K at a heating rate of 10 K/min (b).

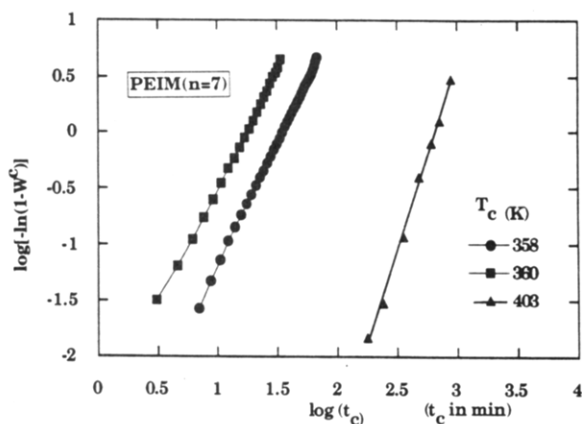


Figure 12. Avrami treatment of PEIM($m=7$).

minutes. The second process then follows. Only one exothermic transition process is found in PEIM($m=7$), and it corresponds to the liquid crystal transition below T_d . Furthermore, the transition kinetics slows down with decreasing isothermal temperature. The slopes of these relationships in Figures 12 and 13 all surprisingly fall into the range of around 2 for the liquid crystal transition process and between 2 and 3 for the crystallization process. However, explanation of these slope values is not unique and straightforward since, without additional morphological information and microscopic kinetic model, the Avrami

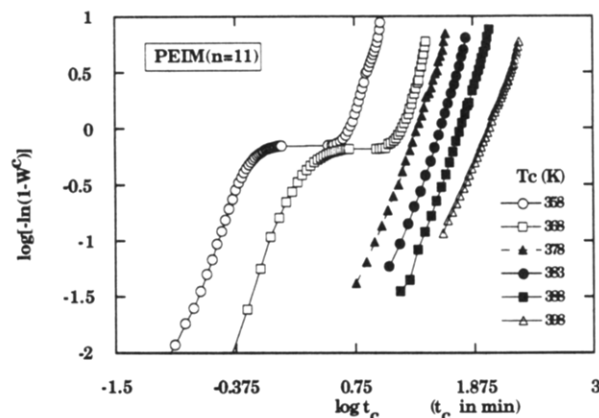


Figure 13. Avrami treatment of PEIM($m=11$).

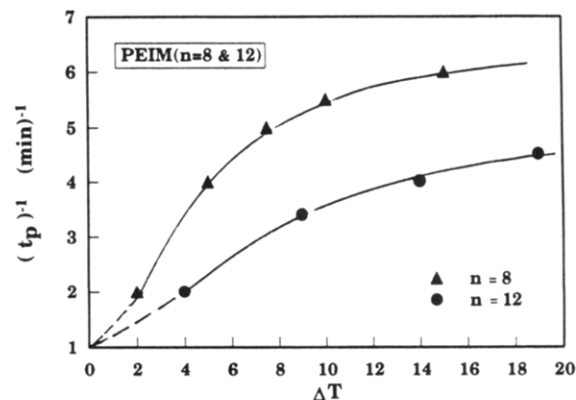


Figure 14. Relationships between $(t_p)^{-1}$ and ΔT for PEIM($m=8$ and 12).

treatment is only a simple representation of experimental transition kinetics data.^{11,35-37}

One may assume that the transition is nucleation-controlled and meets the requirements of the Avrami treatment¹⁴ as in the kinetic studies of small-molecule liquid crystals.³⁸⁻⁴⁰ The slope thus represents the dimensionality of the phase morphology. Nevertheless, the concept of nucleation in this kind of transition might deviate from the classical meaning which possesses a surface free energy barrier to be overcome with a critical nucleation size. Instead, it is likely that in a liquid crystal transition a local site having a relatively low Gibbs free energy due to the energy (and density) fluctuation(s) caused by molecular motion may act as a center of the further development (aggregation) of the liquid crystal phase. The energy barrier in this case must be small when the molecular motion is fast enough.

To quantitatively study the liquid crystal transition kinetics, we take the peak time to represent the measure of the transition rate, t_p . The reason for this choice is due to the fast kinetics for some of the polymers, and only the peak times can be precisely determined during the experimental equilibration. Experimentally, this time is close to 50% of the conversion to the ordered phase. Therefore, one may plot relationships between $(t_p)^{-1}$ and supercooling ($\Delta T = T_d - T_c$) as illustrated in Figures 14 and 15a,b for PEIM($m=8$ and 12) and PEIM($m=7, 9$, and 11), respectively. Note that $(t_p)^{-1}$ is proportional to the transition rate. With increasing the number of methylene units in the spacer, the transition kinetics becomes slower at constant undercooling. Furthermore, except for PEIM($m=7$), with increasing supercooling the transition kinetics speeds up, indicating that the barrier to hamper this kinetics decreases. In PEIM($m=7$) (Figure 15a), the transition time increases (hence the rate decreases) with

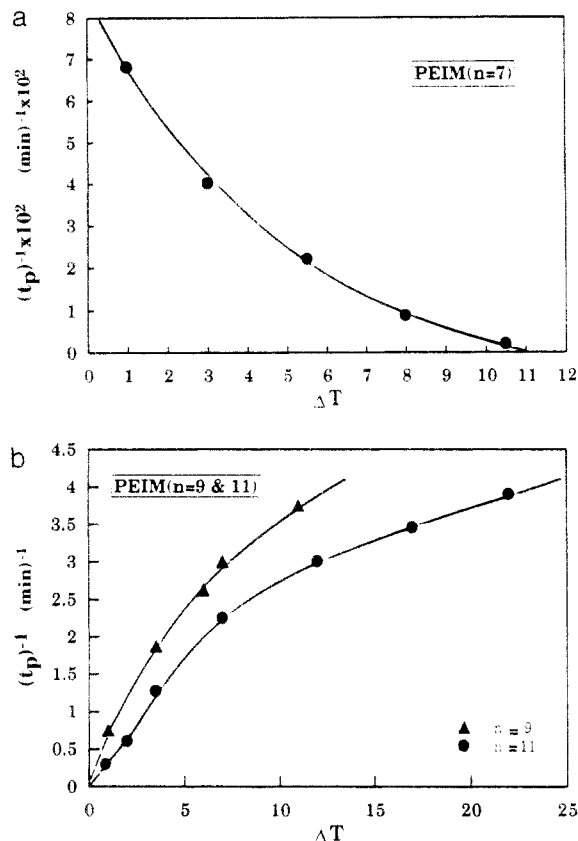


Figure 15. Relationships between $(t_p)^{-1}$ and ΔT for PEIM($m=7$) (a) and PEIM($m=9$ and 11) (b).

supercooling. This is due to the fact that here T_d approaches T_g , and the temperature range available for the study of the transition process is entirely dominated by chain mobility and thus by transport. In fact, the highest measurable rate is that at 360 K (Figures 4 and 5), which is virtually at T_d itself (see Table 2).

If one uses the absolute reaction rate theory put forward by Turnbull and Fisher⁴¹ to describe the transition rate after a modification under the assumption that the overall phase transition rate is proportional to the term of $(t_p)^{-1}$ obtained from the experimental data, one may obtain

$$\ln(t_p)^{-1} = \ln G_0 - (\Delta G_\eta + \Delta G^*)/kT \quad (1)$$

Here, ΔG^* stands for the Gibbs free energy of the transition barrier, ΔG_η represents the activation free energy which governs the short distance diffusion of the segments as a transport term, and G_0 is a statistical prefactor which is associated with both the Planck and Boltzmann constants. The transition barrier term increases with decreasing supercooling when the temperature approaches the transition temperature. The transport term is, however, only active when the temperature is close to the glass transition temperature where the cooperative molecular motion stops. The detailed expression of the transition barrier is given by

$$\Delta G^*/kT = KT_d/(kT\Delta H_d\Delta T) \quad (2)$$

where K represents an energy barrier term which needs to be overcome in a transition process. ΔH_d is the liquid crystalline transition enthalpy as listed in Table 2, and ΔT is supercooling ($T_d - T$). The transport term can be considered as a WLF type equation. For PEIM($m=7$), one assumes that the ΔG^* term is constant and small when the temperature is close to T_g , and only the ΔG_η term

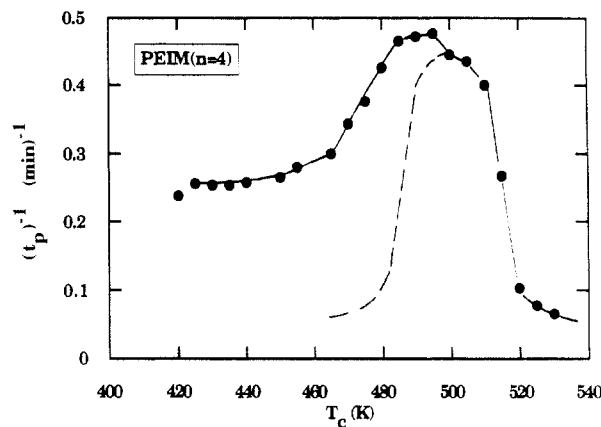


Figure 16. Relationship between $(t_p)^{-1}$ and temperature for PEIM($m=4$).

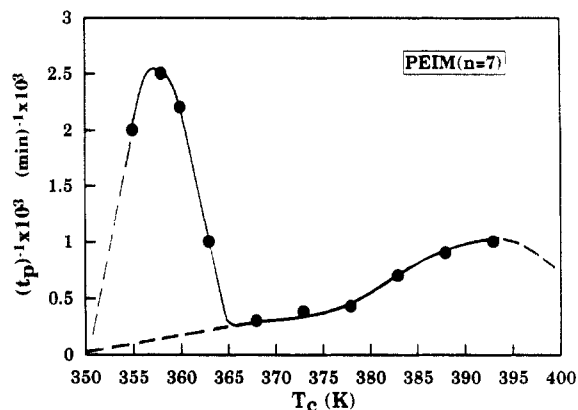


Figure 17. Relationship between $(t_p)^{-1}$ and temperature for PEIM($m=7$).

affects the transition kinetics. If one plots $\ln(t_p)^{-1}$ versus reciprocal $(T - 309.4 \text{ K})$, the slope should be proportional to the transport term ΔG_η . From calculations, this value is 6.4 kJ/mol, which is remarkably close to the universal value of 6.28 kJ/mol proposed by Hoffman et al.⁴² If one further assumes that this value may be used to describe all the PEIMs, the relationships between $\ln(t_p)^{-1} + \Delta G_\eta/(T - T_\infty)$ versus reciprocal $(T\Delta T)$ yield the energy barrier terms (proportional to the slopes) for PEIMs. The ratios of other PEIMs to PEIM($m=8$) (as a reference) are 1.2 for PEIM($m=9$), 1.4 for PEIM($m=11$), and 1.5 for PEIM($m=12$), indicating a slight increase of the energy barrier with increasing methylene units. Note that these values only possess relative meanings as in comparison to other PEIMs.

Crystallization Kinetics from both the Isotropic Melt and the Liquid Crystal Phase. Many aspects can be raised to discuss the crystallization kinetics in PEIMs. We only focus on the effect of the preexisting liquid crystal phase on the crystallization process. Furthermore, since two different ordered structures (forms I and II) have been found in PEIM($m=6, 8, 10$, and 12), the crystallization kinetics may differ for these two structures. As a result, only PEIM($m=4$) and PEIM($m=\text{odd}$)s are studied in this present report, in which only one crystal structure is observed for each polymer. Figures 16–18 show the relationships between $(t_p)^{-1}$ and temperature over the whole crystallization temperature range (both below and above T_d). The kinetics of both the liquid crystal formation and crystallization are included. Generally speaking, except in the vicinity of T_d (see below), the formation of the liquid crystal phase is faster than that of the crystals. This leads to a case where the liquid crystalline phase forms first below T_d , and the later crystallization is then

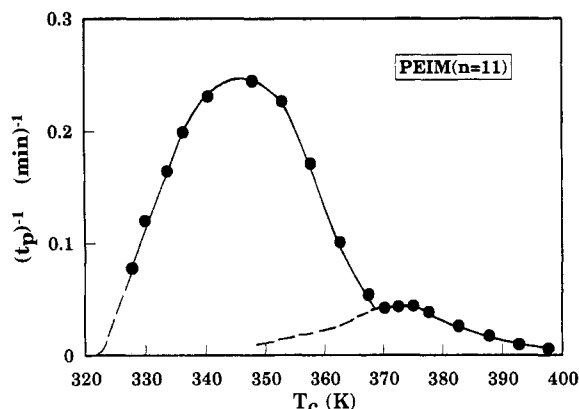


Figure 18. Relationship between $(t_p)^{-1}$ and temperature for PEIM($m=11$).

affected by this liquid crystal ordering. For PEIM($m=4$) (Figure 16), above $T_d = 500$ K, the overall crystallization rate increases with increasing supercooling, as is usually expected. In this temperature (supercooling) region, the crystals are formed directly from the isotropic melt. Below T_d (here 500 K), on the other hand, there is an abnormal increase of the overall crystallization rate, in excess to what is expected for crystallization without the existence of the liquid crystal precursor phase, the latter being represented by the dashed line. This effect is observed more predominantly in PEIM($m=11$) as shown in Figure 18. The overall crystallization rate increases by more than 1 order of magnitude below T_d (here 370 K). Even in the case of PEIM($m=7$), Figure 17 indicates that, in a very narrow temperature region of 11 K (here close to $T_d = 361$ K), the liquid crystal phase forms much faster, up to about 1 order of magnitude at the maximum, than the crystal phase (compared to Figure 15a). The differences between the experimentally observed data and the dashed line may reflect the effect of a preexisting liquid crystal phase on the crystallization.

The overall crystallization rate increase due to the preexistence of the liquid crystal phase may be attributed to two factors: an increase of nucleation rate, an increase of crystal growth rate, or both. At this moment, we cannot distinguish one from another since the crystal growth rate has to be known first. Unfortunately, in the PEIM case, we cannot observe any crystalline texture grown from the liquid crystal state under PLM. In a polyether synthesized from 1-(4-hydroxyphenyl)-2-(2-methyl-4-hydroxyphenyl)-ethane and α,ω -dibromoalkanes, crystal spherulites grown from the liquid crystal phase can be observed via PLM (Figure 8a–d in ref 22). In a separate paper on a polyether⁴³ with isothermal temperatures close to T_d , crystal growth, in the form of expanding spherulites, and nucleation through the appearance of new spherulites could be identified individually and the respective rates measured. While revealing new morphological effects of interest in their own right, the morphologically determined rate values did not match quantitatively the calorimetrically obtained data, raising further important issues. Clearly, a comprehensive attack on these problems utilizing the combined experience with the different materials and methods is invited.

At this point, we may have a competition between two transition processes, one leading into crystal and the other into liquid crystal. In the present cases, the former extends over the full temperature range between T_m and T_g , while the latter extends only from T_d downward where $T_d < T_m$. It follows that the liquid crystal, while stable with respect to the melt, is metastable with respect to the crystal which

is the phase of ultimate stability. Competition between such phase formations has received attention recently as part of a more general treatment (Appendix II of ref 44). Under all circumstances, there is an upper temperature interval, here $T_m - T_d$, where only the phase of ultimate stability (here crystal) can arise. At T_d the metastable phase (here liquid crystal) can also appear. Below T_d usually the rate of development of the metastable phase increases much faster on further lowering of temperature than that of the stable phase. This general experience provides a kinetics-based explanation for the otherwise empirical Ostwald's law of successive states.³⁴ As at T_d the rate of metastable phase growth needs to be zero while that of the stable phase has a finite (even if usually still low) value, it follows that the two rates must cross at some temperature $T_x < T_d$. Due to the much faster increase of the liquid crystal formation with ΔT , as in Figures 14 and 15, T_x will only be slightly below T_d , and in the present work, since the much faster increase of the very large disparity of the two rates in that temperature region, T_x could not yet be identified. For this, faster crystallizing polymers would be required.

Conclusion

In this paper, we have studied order sequences observed in monotropic PEIM(m). For PEIM($m=8, 10$, and 12), a crystal phase can be formed directly from the isotropic melt above T_d , while below that temperature, a smectic A liquid crystal phase develops first, followed by a further ordering process to form a structure with a hexagonal-like packing. Only after a prolonged annealing time can the crystal structure recover. PEIM($m=6$) acts as an intermediate polymer compared to PEIM($m=4$) which does not possess the second-ordered structures after the liquid crystal formation. On the other hand, all PEIM($m=\text{odd}$)s show the same crystal structures no matter if they are crystallized below or above T_d . We have demonstrated that, in PEIMs, the liquid crystal transition kinetics from the isotropic melt can be experimentally accessed and investigated. It is particularly interesting that in PEIM($m=7$) the liquid crystal transition kinetics is very slow and the transition rate decreases when the temperature is closer to the glass transition temperature. This is solely due to hampered molecular motion although the transition is thermodynamically close to an equilibrium. For other PEIM($m=\text{odd}$)s, the liquid crystal transition kinetics can also be followed. The effect of a preexisting liquid crystal phase on the crystallization kinetics has been investigated. This leads to an unusual increase of the crystallization rate in the temperature region below T_d , raising new important issues.

Acknowledgment. This work was supported by S.Z.D.C.'s Presidential Young Investigator Award from the National Science Foundation (Grant DMR-9175538).

References and Notes

- (1) For a recent review, see, for example: Percec, V.; Tomazos, D. In *Comprehensive Polymer Science, First Supplement*, Allen, G., Aggarwal, S. L., Russo, S., Eds.; Pergamon: Oxford, U.K., 1992; pp 300–356. In this review, over four hundred references were collected.
- (2) Thomas, E. L.; Wood, B. A. *Faraday Discuss. Chem.* **1985**, *79*, 229.
- (3) Wood, B. A.; Thomas, E. L. *Nature* **1986**, *324*, 655.
- (4) Hudson, S. D.; Vezie, D.; Thomas, E. L. *Makromol. Chem., Rapid Commun.* **1990**, *11*, 657.
- (5) Ciora, R. J.; Magill, J. H. *Macromolecules* **1990**, *23*, 2350, 2359.

- (6) Magill, J. H. In *Integration of Fundamental Polymer Science Technology*; Kleingens, L. A., Lemstra, P. J., Eds.; Elsevier: London/New York, 1988; p 280.
- (7) Grebowicz, J.; Cheng, S. Z. D.; Wunderlich, B. *J. Polym. Sci., Polym. Phys. Ed.* **1986**, *24*, 675.
- (8) Jonsson, H.; Wallgren, E.; Hult, A.; Gedde, U. W. *Macromolecules* **1990**, *23*, 1041.
- (9) Cheng, S. Z. D.; Janimak, J. J.; Lipinski, T. M.; Sridhar, K.; Huang, X.-Y.; Harris, F. W. *Polymer* **1990**, *31*, 1122.
- (10) Campoy, I.; Marco, C.; Gomez, M. A.; Fatou, J. G. *Macromolecules* **1992**, *25*, 4392.
- (11) Cheng, S. Z. D. *Macromolecules* **1988**, *21*, 2475.
- (12) Cheng, S. Z. D.; Zhang, A.-Q.; Johnson, R. L.; Wu, Z.; Wu, H. H. *Macromolecules* **1990**, *23*, 1196.
- (13) Cheng, S. Z. D.; Johnson, R. L.; Wu, Z.; Wu, H. H. *Macromolecules* **1991**, *24*, 150.
- (14) Avrami, M. *J. Chem. Phys.* **1939**, *7*, 1109; **1940**, *8*, 212; **1941**, *9*, 117.
- (15) Lehmann, O. *Über Physikalische Isomerie*; from Keller, H., 1877. History of Liquid Crystals. *Mol. Cryst. Liq. Cryst.* **1973**, *21*, 1.
- (16) Volander, D. *The Investigation of Molecular Shape with the Aid of Liquid Crystals*; communication from the Institute of Chemistry of Halle, ADS, 1923.
- (17) Percec, V.; Tsuda, Y. *Macromolecules* **1990**, *23*, 4347.
- (18) Percec, V.; Yourd, R. *Macromolecules* **1989**, *22*, 524, 3229.
- (19) Ungar, G.; Feijoo, J. L.; Keller, A.; Yourd, R.; Percec, V. *Macromolecules* **1990**, *23*, 244.
- (20) Ungar, G.; Percec, V.; Zuber, M. *Macromolecules* **1992**, *25*, 1193.
- (21) Cheng, S. Z. D.; Yandrasits, M. A.; Percec, V. *Polymer* **1991**, *32*, 1284.
- (22) Yandrasits, M. A.; Cheng, S. Z. D.; Zhang, A.-Q.; Cheng, J.-L.; Wunderlich, B.; Percec, V. *Macromolecules* **1992**, *25*, 2112.
- (23) Cheng, J.-L.; Wunderlich, B.; Cheng, S. Z. D.; Yandrasits, M. A.; Zhang, A.-Q.; Percec, V. *Macromolecules* **1992**, *25*, 5995.
- (24) Chen, J.-H.; Zhang, A.-Q.; Yandrasits, M. A.; Cheng, S. Z. D.; Percec, V. *Makromol. Chem.* **1993**, *194*, 3135.
- (25) Pardey, R.; Harris, F. W.; Cheng, S. Z. D.; Aducci, J.; Facinelli, J. V.; Lenz, R. W. *Macromolecules* **1992**, *25*, 5060.
- (26) Pardey, R.; Harris, F. W.; Cheng, S. Z. D.; Aducci, J.; Facinelli, J. V.; Lenz, R. W. *Macromolecules* **1993**, *26*, 3687.
- (27) Pardey, R. Ph.D. Dissertation, Department of Polymer Science, The University of Akron, Akron, OH, 1993.
- (28) de Abajo, J.; de la Campa, J.; Kricheldorf, H. R.; Schwarz, G. *Makromol. Chem.* **1990**, *191*, 537.
- (29) Kricheldorf, H. R.; Huner, R. *Makromol. Chem., Rapid Commun.* **1990**, *11*, 211.
- (30) Kricheldorf, H. R.; Domschke, A.; Schwarz, G. *Macromolecules* **1991**, *24*, 1011.
- (31) Kricheldorf, H. R.; Jahnke, P. *Eur. Polym. J.* **1990**, *9*, 1009.
- (32) Kricheldorf, H. R.; Schwarz, G.; de Abajo, J.; de la Campa, J. *Polymer* **1991**, *32*, 942.
- (33) Kricheldorf, H. R.; Huner, R. *J. Polym. Sci., Polym. Chem. Ed.* **1992**, *30*, 337.
- (34) Ostwald, W. Z. *Phys. Chem.* **1897**, *22*, 286.
- (35) Cheng, S. Z. D.; Wunderlich, B. *Macromolecules* **1988**, *21*, 3327.
- (36) Schultz, J. *Polymer Materials Science*; Prentice-Hall: Englewood Cliffs, NJ, 1974.
- (37) Wunderlich, B. *Macromolecular Physics, Crystal Nucleation, Growth, Annealing*; Academic: New York, 1976; Vol. II, Chapter 6.
- (38) Jabarin, S. A.; Stein, R. S. *J. Phys. Chem.* **1973**, *77*, 409.
- (39) Price, F. P.; Wendorff, J. H. *J. Phys. Chem.* **1971**, *75*, 2839, 2849; **1972**, *76*, 276.
- (40) Price, F. P.; Fritzsdche, A. K. *J. Phys. Chem.* **1973**, *77*, 396.
- (41) Turnbull, D.; Fisher, J. C. *J. Chem. Phys.* **1949**, *17*, 71.
- (42) Hoffman, J. D.; Davis, G. T.; Lauritzen, J. I., Jr. In *Treatise of Solid State Chemistry*; Hannay, N. B., Ed.; Plenum Press: New York, 1976; Vol. III, Chapter 7.
- (43) Heberer, D. P.; Keller, A.; Percec, V., in preparation.
- (44) Keller, A.; Hikosaka, M.; Rastogi, S.; Toda, A.; Berham, P. J.; Goldbeck-Wood, G. *J. Mater. Sci.* **1994**, *29*, 2579.